FOCUSED TOPIC

Can Eco-Evo Theory Explain Population Cycles in the Field?*

Greg Dwyer,[1,†] Joseph R. Mihaljevic,[2] and Vanja Dukic[3]

1. Department of Ecology and Evolution, University of Chicago, Chicago, Illinois 60637; 2. School of Informatics, Computing, and Cyber Systems, Northern Arizona University, Flagstaff, Arizona 86011; 3. Department of Applied Mathematics, University of Colorado, Boulder, Colorado 80309

Submitted March 26, 2020; Accepted February 25, 2021; Electronically published November 22, 2021

Online enhancements: appendix.

ABSTRACT: Efforts to explain animal population cycles often invoke consumer-resource theory, which has shown that consumer-resource interactions alone can drive population cycles. Eco-evo theory instead argues that population cycles are partly driven by fluctuating selection for resistance in the resource, but support for eco-evo theory has come almost entirely from laboratory microcosms. Here we ask, Can eco-evo theory explain population cycles in the field? We compared the ability of eco-evo models and classical "eco-only" models to explain data on cycles in the insect *Lymantria dispar*, in which outbreaks of the insect are terminated by a fatal baculovirus. We carried out a statistical comparison of the ability of eco-only and eco-evo models to explain combined data from *L. dispar* outbreak cycles and baculovirus epizootics (epidemics in animals). Both models require high host variation in resistance to explain the epizootic data, but high host variation in the eco-evo model leads to consistently accurate predictions of outbreak cycles, whereas in the presence of high host variation the eco-only model can explain outbreak cycles only by invoking high levels of stochasticity, which leads to highly variable and often inaccurate predictions of outbreak cycles. Our work provides statistically robust evidence that eco-evo models can explain population cycles in the field.

Keywords: eco-evo, host-pathogen, population cycle, insect outbreak, statistical computing.

Introduction

Ecologists have struggled for almost a century to provide mechanistic explanations for animal population cycles (Elton 1924). The most widely cited explanations come from consumer-resource theory, which has shown that population cycles can be driven by predator-prey and host-pathogen interactions (Kot 2001), but alternative theories have shown that cycles can also be driven by environmental stochasticity, age or stage structure, and consumer-induced changes in resource quality (Barraquand et al. 2017). Here we test an important recent alternative to classical consumer-resource theory: eco-evolutionary (or "eco-evo") consumer-resource theory (Ellner 2013).

Eco-evo theory was developed in response to empirical evidence showing that evolutionary change often occurs rapidly enough to affect ecological change (Duffy and Sivars-Becker 2007; Hanski 2011; Ohlberger et al. 2011; Toju 2011; Duffy et al. 2012; Bruijning et al. 2019). Because evolutionary biologists had long believed that evolutionary change could only occur slowly, the change of perspective that has resulted from observations of rapid evolutionary change has been sufficiently revolutionary that it has been referred to as "a paradigm shift" (Reznick et al. 2019).

Eco-evo consumer-resource theory postulates that population cycles are driven by feedbacks between ecological and evolutionary mechanisms (Govaert et al. 2019), whereas classical "eco-only" consumer-resource theory includes only ecological mechanisms. In eco-only consumer-resource theory, peaks in the density of the resource are terminated by high densities of the consumer; the resulting decline in the resource leads to a decline in the consumer, which in turn permits a resurgence in the resource and thus sustained cycles (Kot 2001). In the best-known version of eco-evo consumer-resource theory, cycles again result from reciprocal changes in consumer and resource densities, but the resource has heritable resistance to consumer attacks, and it experiences a trade-off between resistance and fecundity (Govaert et al. 2019). High consumer densities then select for increased resource resistance, exacerbating the decline in the consumer that results from a reduction in the density of the resource. Low consumer densities instead select

* This contribution is part of a Focused Topic organized by Bret Elderd, Nicole Mideo, and Meghan Duffy featuring studies bridging across scales in disease ecology and evolution.

† Corresponding author; email: gdwyer@uchicago.edu.

ORCID: Dwyer, https://orchid.org/0000-0002-7387-2075; Mihaljevic, https://orchid.org/0000-0003-2320-5773.

  https://doi.org/10.1086/717178

for increased resource fecundity, speeding the resurgence in the resource that results from a reduction in the density of the consumer.

These differences are important because eco-evo models can produce qualitatively different predictions than classical eco-only models. In some eco-evo models peaks in consumer and resource densities are out of phase, lagging each other by half a cycle period, compared with the quarter-cycle lag of classical eco-only models (Yoshida et al. 2003; Cortez and Ellner 2010). Eco-evo theory may thus revamp our understanding of consumer-resource cycles.

Empirical support for eco-evo consumer-resource theory, however, relies almost entirely on laboratory microcosms. This reliance has been documented in a review by Hendry (2019); the effect, Hendry argues, is that eco-evo consumer-resource theory has little to no support from "the real world," meaning from the field as opposed to from the laboratory. The importance of Hendry's criticism is indirectly illustrated by a second review, which argues for the generality of out-of-phase consumer-resource cycles by citing only laboratory microcosm studies (Hiltunen et al. 2014). A focus on laboratory microcosms is also apparent in a reanalysis of a broad range of eco-evo models, in which seven out of nine reanalyzed models had been constructed from laboratory microcosm data, while the remaining two models had been constructed from laboratory experiments that used field-collected organisms (Cortez et al. 2020). The focus on laboratory data is a problem because field ecologists have known for decades that laboratory studies often give different results than field studies (Carpenter 1996). Eco-evo theory has therefore received only passing mention by theoretical ecologists (Barraquand et al. 2017) while often being ignored altogether by empirical ecologists (Moreau et al. 2018; Myers 2018; Oli 2019).

Here we therefore ask, Is eco-evo theory useful for explaining animal population cycles in the field? To answer this question, we tested whether eco-evo models can explain field data for an outbreaking insect, the moth *Lymantria dispar*.[1] Modern approaches to model testing emphasize the use of data to choose between alternative models (Burnham and Anderson 2002), so we allowed for the possibility that the data are better explained by eco-only models. We therefore tested whether eco-evo models provide a quantitatively better explanation for the data than eco-only models.

Part of the reason why it was important to quantitatively compare eco-evo and eco-only models is that eco-only models have a long history of providing reasonable explanations for population cycles in forest-defoliating insects (Varley et al. 1973; Anderson and May 1980). In *L. dispar* and other forest defoliators, population peaks are terminated by natural enemies, typically parasitoids and pathogens (Myers 1988; Roland and Taylor 1997; Moreau and Lucarotti 2007), including the *L. dispar* baculovirus, which we study here (Woods and Elkinton 1987). Eco-only consumer-resource models show behavior that qualitatively matches this pattern; in both models and data, population peaks in the resource are terminated by the consumer (Dwyer et al. 2000; Cobbold et al. 2009), and the host insect shows long-period (6–10 years), large-amplitude (four to five orders of magnitude) fluctuations in density (Varley et al. 1973; Myers 1988).

It is nevertheless true that, as assumed in eco-evo models, baculoviruses and other pathogens impose severe selection on their insect hosts for increased resistance, and insect resistance to baculoviruses and other pathogens is often heritable (Fuxa and Tanada 1987). The lack of mention of eco-evo models in the forest-defoliator literature (Johns et al. 2016; but see Cory and Myers 2009) is therefore likely due to the qualitative successes of eco-only models at explaining defoliator data (Hunter and Dwyer 1998), combined with the greater conceptual simplicity of eco-only models (as we will discuss, eco-evo insect outbreak models do not show out-of-phase cycles, so using qualitative comparisons to distinguish between eco-only and eco-evo models may be possible only for microcosm models). Here we instead argue that when two theories provide qualitative predictions that are equally successful, what is needed are quantitative comparisons of models to data (Luo and Koelle 2013). This issue is of course not restricted to studies of forest-defoliating insects; indeed, it is unclear whether there are any field data on animal population cycles that cannot be qualitatively explained by eco-only models (Turchin 2003), suggesting that quantitative comparisons of models to data are a general necessity for testing eco-evo theory.

In the case of forest-defoliating insects, however, an important problem is that data sets on insect outbreak cycles almost always track only the insect (Varley et al. 1973; Myers 1988), whereas eco-only models track both the insect and the pathogen; additionally, eco-evo models track host resistance. It is thus unlikely that insect outbreak data on their own would be enough to allow us to quantitatively choose between eco-evo and eco-only models. Analyses of insect outbreak data have therefore instead often relied on time-series models (Moreau and Lucarotti 2007; Johns et al. 2016). In such analyses, second-order lags in partial autocorrelation functions, a standard output of time-series software, are taken as qualitative support for eco-only models, following Turchin's (1990) observation that second-order lags are characteristic of consumer-resource interactions. Time-series analyses are more statistically robust than

1. This insect's common name in English was "gypsy moth," but that name is an ethnic slur and is therefore no longer in use; a new English common name has not yet been selected.

qualitative comparisons of models to data but exclude eco-evo models from consideration altogether.

To quantitatively compare eco-evo models and eco-only models, we therefore used more than just long-term time-series data from *L. dispar* outbreaks; instead, we first fitted some model parameters to short-term time-series data from baculovirus epizootics (epizootics are epidemics in animals) in *L. dispar* populations (Woods and Elkinton 1987) before fitting the remaining parameters to long-term data from *L. dispar* outbreaks (Skaller 1985; Williams et al. 1991; Ostfeld et al. 1996). To approach the high level of causal inference achieved by experimental microcosm studies, we also used data from baculovirus field experiments, in the form of informative Bayesian priors on key model parameters (Elderd et al. 2008; Fuller et al. 2012; Fleming-Davies et al. 2015; Páez et al. 2017). We then chose between the eco-evo and eco-only models using the Watanabe-Akaike information criterion (WAIC), a Bayesian model selection criterion (Gelman et al. 2014).

Field experiments had previously shown that, as assumed by eco-evo models, an *L. dispar* individual's resistance to the baculovirus is highly variable and partly heritable and that resistance has a fitness cost (Elderd et al. 2006; Páez et al. 2017). Moreover, in standard eco-evo insect outbreak models, heritable but costly host resistance leads to realistic cycles (Elderd et al. 2006; Páez et al. 2017), whereas in the corresponding eco-only insect outbreak models highly variable host resistance leads to an unrealistic stable equilibrium (Dwyer et al. 2000). The experimental data thus support eco-evo models over eco-only models.

The field experiments in question, however, were carried out on single branches for 1 week, whereas *L. dispar* outbreaks encompass hundreds of square kilometers (Liebhold and Kamata 2000) and last for years (Johnson et al. 2005). The field experiments were thus carried out at smaller spatial scales and shorter timescales than the scales at which *L. dispar* outbreaks occur in nature. Eco-evo models of insect outbreaks are therefore subject to the same criticism that Hendry (2019) leveled at eco-evo models in general: the models have not been tested with data from the real world. Moreover, stochasticity can turn the unrealistic damped cycles of deterministic eco-only models into realistic sustained cycles (Nisbet and Gurney 2003); stochastic eco-only models could therefore provide an explanation for *L. dispar* outbreak cycles that is as good or better than the explanation provided by eco-evo models.

As we will show, however, *L. dispar* outbreak cycles are better explained by eco-evo models. Our work thus provides what is to our knowledge the first statistically robust evidence that eco-evo dynamics drive population cycles in the field. Because our models also include substantial delays between infection and infectiousness (Kennedy et al. 2014), which lead to a type of stage structure, our work demonstrates that stage structure also has a key role to play in consumer-resource cycles. As we discuss, our work has implications for the use of baculoviruses in pest control (Webb et al. 2005).

Methods

A Model of Baculovirus Epizootics

In defoliating insects like *Lymantria dispar*, baculovirus transmission occurs when host larvae feed on foliage contaminated with viral particles released from infectious cadavers (Cory and Myers 2003). Baculoviruses must therefore kill to be transmitted, and only larvae can become infected. Epizootics can be terminated by host pupation, but they can also be terminated by the decimation of the host population by the baculovirus (Fuller et al. 2012). Hosts that survive the epizootic reproduce in the late summer after transmission has ended.

As is often true of insect baculoviruses (Fuller et al. 2012), the *L. dispar* baculovirus overwinters largely through the external contamination of egg masses, which leads to infections among hatchlings (Murray and Elkinton 1989, 1990). Because multiple rounds of transmission occur after hatch, baculovirus infection rates increase strongly with host density (Woods et al. 1991), as is also often true for insect baculoviruses (Moreau and Lucarotti 2007). Since the introduction of the fungal pathogen *Entomophaga maimaiga* in 1989, *L. dispar* outbreaks have been less frequent and less severe in North America (Tobin et al. 2012), so baculovirus epizootics have almost entirely ceased (Kyle et al. 2020). *Entomophaga maimaiga* prefers moderate temperatures, however, so climate change may be shifting the competitive balance back to the baculovirus (Elkinton et al. 2019). Here we therefore consider *L. dispar*–baculovirus dynamics in the pre–*E. maimaiga* period.

Because host variation strongly modulates baculovirus epizootics in *L. dispar* populations (Dwyer et al. 1997), host variation is a key feature of our epizootic model. The epizootic model, however, describes baculovirus spread during only a single larval season, so host reproduction is instead incorporated into the eco-only and eco-evo models that describe long-term dynamics (Dwyer et al. 2000). Assumptions about whether host variation in resistance is genetic or environmental are thus relevant only for the long-term models, so our eco-evo and eco-only models use the same epizootic model.

The epizootic model is a susceptible-exposed-infectious-removed (SEIR) model from human epidemiology (Keeling and Rohani 2008), where S is the symbol for susceptible, E is the symbol for exposed, I is the symbol for infectious, and R is the symbol for removed. Because in our case the infectious class consists of pathogen-killed

cadavers, we use P instead of I, and we do not use R because a removed class would represent cadavers that are no longer infectious and that are therefore of no interest. In addition to these changes in symbols, we also changed the model structure to include host variation in infection risk (Dwyer et al. 2000):

$$\overbrace{\frac{dS}{dt}}^{\text{change in susceptible hosts}} = -\overbrace{\underbrace{\bar{\nu}}_{\substack{\text{initial}\\ \text{average}\\ \text{transmission}}}\left(\frac{S(t)}{S(0)}\right)^{C^2}}^{\substack{\text{average}\\ \text{transmission}\\ \text{at time } t}}\underbrace{S}_{\substack{\text{host}\\ \text{density}}}\underbrace{P}_{\substack{\text{pathogen}\\ \text{density}}}, \tag{1}$$

$$\overbrace{\frac{dE_1}{dt}}^{\substack{\text{change in}\\ \text{exposed-host}\\ \text{class 1}}} = \bar{\nu}SP\left(\frac{S(t)}{S(0)}\right)^{\overbrace{C^2}^{\substack{\text{CV of}\\ \text{transmission}}}} - \overbrace{\underbrace{m}_{\substack{\text{no. of}\\ \text{exposed}\\ \text{classes}}}\underbrace{\delta}_{\substack{\text{death}\\ \text{rate}}}E_1}^{\substack{\text{aging into}\\ \text{next exposed}\\ \text{class}}}, \tag{2}$$

$$\overbrace{\frac{dE_i}{dt}}^{\substack{\text{change in}\\ \text{exposed}\\ \text{class } i}} = \overbrace{m\delta E_{i-1}}^{\substack{\text{aging out of}\\ \text{previous class}}} - \overbrace{m\delta\underbrace{E_i}_{\substack{\text{hosts in}\\ \text{exposed}\\ \text{class } i}}}^{\substack{\text{aging into}\\ \text{next class}}}\overbrace{(i = 2, \ldots, m)}^{\text{all but class 1}}, \tag{3}$$

$$\overbrace{\frac{dP}{dt}}^{\substack{\text{change in}\\ \text{infectious}\\ \text{cadavers}}} = \overbrace{m\delta E_m}^{\substack{\text{death of}\\ \text{hosts in final}\\ \text{exposed class}}} - \overbrace{\underbrace{\mu}_{\substack{\text{decay}\\ \text{rate}}}P}^{\substack{\text{cadaver}\\ \text{decay}}}. \tag{4}$$

Because the model includes multiple exposed classes, it allows for a gamma-distributed delay between infection and death (Keeling and Rohani 2008); for brevity in what follows, we refer to the length of this delay as the "speed of kill." More complex models allow for "fat-tailed" distributions of speed of kill, in which some infected hosts take a long time to die (Wearing et al. 2005), but allowing for this complication is beyond the scope of our work.

The mean speed of kill in the model is the inverse of the death rate $1/\delta$, while the variance in the speed of kill is $1/m\delta^2$ (Keeling and Rohani 2008). Increases in the number of exposed classes m thus reduce the variance in the speed of kill, which in turn has important consequences for outbreaks. To explain these consequences, we note first that the variance in the speed of kill of infected hatchlings is very low (Woods and Elkinton 1987), so we assume that infected hatchlings all die at the same time after hatch. The death of the infected hatchlings then creates a sharp initial pulse of infectious cadavers. If the variance in the speed of kill of later-stage larvae is also low, the initial pulse will lead to additional pulses later in the epizootic; the last few pulses, however, may be eliminated if the epizootic is terminated by host pupation.

The elimination of the last few pulses in turn means that multiple generations may be required for the pathogen to decimate the host, creating a delay between the peak density of the insect and the peak density of the pathogen. A low variance in the speed of kill thus increases the severity of the delayed density dependence imposed by the pathogen, which in turn increases the period and amplitude of the host-pathogen population cycle (Krylova and Earn 2013). Because these effects are caused by pulses in the infection rate, they are a consequence of a type of stage structure.

The parameter $\bar{\nu}$ is the average transmission rate, the rate at which uninfected hosts become infected by (accidentally) feeding on dead infectious cadavers. The distribution for which $\bar{\nu}$ is the mean has coefficient of variation C, the ratio of the standard deviation to the mean (for the purposes of fitting the SEIR models to data, we reparameterized according to $k = 1/C^2$; estimating k instead of C improves normality, thereby producing more robust inferences; see Mihaljevic et al. 2020). Because $\bar{\nu}$ is a measure of infection risk, we use it as an inverse measure of host resistance. For brevity we refer to $\bar{\nu}$ as "average risk," but strictly speaking $\bar{\nu}$ is the average risk only at the beginning of the epizootic.

The average risk for time $t > 0$ is instead $\bar{\nu}(S(t)/S(0))^{C^2}$, where $S(0)$ is the initial host density and $S(t)$ is the host density at t (Dwyer et al. 2000). Given that there is no host reproduction during the epizootic, the density of uninfected hosts $S(t)$ declines as the epizootic proceeds. Average risk therefore also declines as the epizootic proceeds because higher-risk hosts become infected and die earlier than lower-risk hosts, but average risk is further reduced by increases in host variation C. This latter effect occurs because increases in C are equivalent to the addition of hosts with both higher than average risk and lower than average risk, but the addition of hosts with lower than average risk has a bigger effect on average risk than the addition of hosts with higher than average risk (Anderson and May 1992).

In the model, a host's infection risk is assumed to be fixed over its lifetime; if infection risk instead varied randomly

over the host's lifetime, variation in risk would be averaged out of the model altogether (Dwyer et al. 1997). Meanwhile, models with no variation in risk provide a poor fit to epizootic data (Dwyer and Elkinton 1993) and are therefore of little interest.

Modeling Insect Outbreak Cycles

Like many outbreaking insects (Hunter 1995), *L. dispar* has discrete, nonoverlapping generations, so we model long-term insect-baculovirus dynamics using difference equations (Briggs and Godfray 1996). To calculate the fraction infected in the long-term models, we nest the within-season SEIR model inside the difference equations (Dwyer et al. 2000). The eco-only and eco-evo models thus differ only in terms of whether they assume that host variation in infection risk is heritable.

Eco-Only Model. In the eco-only model, host variation in infection risk is assumed to be due entirely to environmental factors and is thus not heritable. Nonheritable host variation in infection risk could be due, for example, to variation in the extent to which an adult female provisions its eggs, which in *L. dispar* can result from variation in the amount of food that was available to that female when it was a larva (Diss et al. 1996). If egg provisioning affects infection risk, variation in a female's nutrition could create environmental variation in its offspring's infection risk.

An individual's infection risk in the eco-only model is further assumed to be uncorrelated with the infection risk of its parents or ancestors; the model thus assumes not only that infection risk is not heritable but also that infection risk has no memory. The mean infection risk $\bar{\nu}$ and the coefficient of variation of infection risk C are therefore constant over generations. Because the average infection risk in the within-season SEIR model falls during the epizootic, infection risk in the eco-only model is reset to the same value at the beginning of each epizootic. The model is then (Dwyer et al. 2000);

$$\overbrace{N_{n+1}}^{\text{hosts in generation } n+1} = \overbrace{\lambda_n}^{\text{fecundity in gen'n } n} \overbrace{N_n}^{\text{hosts in gen'n } n} \overbrace{(1 - i(N_n, Z_n))}^{\text{fraction surviving epizootic}}, \tag{5}$$

$$\overbrace{Z_{n+1}}^{\text{cadavers in generation } n+1} = \overbrace{\phi}^{\text{over-wintering}} N_n \overbrace{i(N_n, Z_n)}^{\text{fraction infected in epizootic}} + \overbrace{\gamma}^{\text{long-term survival}} \overbrace{Z_n}^{\text{cadavers in gen'n } n}. \tag{6}$$

Because *L. dispar* population growth may be affected by stochastic fluctuations in weather (Williams and Liebhold 1995), we allow fecundity λ_n to vary stochastically across generations n, following a lognormal distribution with constant mean and variance. Infectious cadavers produced during the epizootic overwinter at rate ϕ; because ϕ allows for both overwinter survival and the high susceptibility of hatchling larvae, it is possible, and indeed likely, that $\phi \gg 1$ (Fuller et al. 2012; Fleming-Davies and Dwyer 2015). The survival of pathogen particles from earlier epizootics is symbolized as γ.

Density dependence enters into the model through the infection rate function $i(N_n, Z_n)$, which is calculated using the within-season SEIR model equations (1)–(4) according to

$$i(N_n, Z_n) \equiv 1 - \frac{S(T)}{S(0)}. \tag{7}$$

Here $S(T)$ is the density of uninfected hosts in the SEIR model at the end of an epizootic that lasts T days. Larval periods typically last 8 weeks (appendix, available online), so we assume that $T = 56$ days. Larval periods also sometimes last 9 or, more rarely, 10 weeks, but Fuller et al. (2012) showed that increasing the epizootic length from 56 to 200 days leads to only modest increases in the infection rate $i(N_n, Z_n)$. Increasing the epizootic period to 9 or 10 weeks would therefore likely have had little effect on our results.

To complete the connection between the within-season SEIR model and the long-term eco-only model, we set the initial host and pathogen densities $S(0)$ and $P(0)$ in the SEIR model equal to the host and pathogen densities N_n and Z_n in the eco-only model:

$$S(0) = N_n, \tag{8}$$

$$P(0) = Z_n. \tag{9}$$

High values of N_n and Z_n in the eco-only model are thus translated into high values of $S(0)$ and $P(0)$ in the SEIR model, in turn leading to a high infection rate $i(N_n, Z_n)$ that causes the host population to crash. After a crash it takes multiple generations for another host outbreak to occur; because of the delays that we referred to earlier, it takes at least a generation after the outbreak peak for the pathogen to reach levels high enough to terminate a host outbreak. The lag between the host and the pathogen peaks leads to the delayed density dependence that drives realistic insect outbreak cycles, as in classical predator-prey models (Kot 2001).

As we described, however, high host variation C lowers the infection rate $i(N_n, Z_n)$, reducing the severity of the delayed density dependence. Indeed, if model epizootics are always terminated by low host densities instead

of by host pupation (Keeling and Rohani 2008), $C > 1$ guarantees a stable point equilibrium in the deterministic eco-only model (Dwyer et al. 2000), following the "$\mathrm{CV}^2 > 1$ rule" of discrete-generation host-parasite models (Hassell et al. 1991). In our model epizootics can instead be terminated by pupation, but $C > 1$ again leads to a stable point equilibrium in deterministic versions of the model (Fuller et al. 2012). Stochasticity nevertheless turns the damped cycles of the deterministic versions of the model into sustained cycles, as generally occurs in models that show damped cycles (Nisbet and Gurney 2003).

Eco-Evo Model. As we mentioned, however, week-long branch-scale field experiments strongly support eco-evo models. First, an experiment using half-sibling *L. dispar* larvae showed that male parents have a meaningful effect on larval infection risk, demonstrating that resistance is heritable (Páez et al. 2017). Heritability in the experiment was $b = 0.13$, with confidence bounds that do not include zero. Additional experiments showed that infection risk is lower in larvae whose parents have survived population crashes, consistent with selection for increased resistance (Elderd et al. 2008). A final field experiment showed that full sibling groups that have lower infection risk have lower fecundity, demonstrating that resistance is costly (Páez et al. 2017).

Allowing for these complications produces our eco-evo model (Páez et al. 2017):

$$N_{n+1} = N_n[1 - i(N_n, Z_n, \bar{\nu}_n)] \times \overbrace{\{r_n + r_n s\bar{\nu}_n[1 - i(N_n, Z_n, \bar{\nu}_n)]^{C^2}\}}^{\text{effect of trade-off on host fecundity}}, \tag{10}$$

$$Z_{n+1} = \phi N_n i(N_n, Z_n, \bar{\nu}_n) + \gamma Z_n, \tag{11}$$

$$\bar{\nu}_{n+1} = \overbrace{\bar{\nu}_n[1 - i(N_n, Z_n, \bar{\nu}_n)]^{bC^2}}^{\substack{\text{avg. genotypic infection} \\ \text{risk at epizootic end}}} \times \frac{\overbrace{\{1 + s\bar{\nu}_n(bC^2 + 1)[1 - i(N_n, Z_n, \bar{\nu}_n)]^{bC^2}\}}^{\text{effect of trade-off on infection risk}}}{\underbrace{1 + s\bar{\nu}_n[1 - i(N_n, Z_n, \bar{\nu}_n)]^{bC^2}}_{\text{normalization factor}}}. \tag{12}$$

To connect the long-term eco-evo model to the within-season SEIR model, we use equations (7)–(9) from the eco-only model, but we add an equation for infection risk:

$$\bar{\nu} = \bar{\nu}_n. \tag{13}$$

Here $\bar{\nu}$ is the initial average infection risk in the within-season SEIR model, while $\bar{\nu}_n$ is the average infection risk in generation n in the eco-evo model. Changes in $\bar{\nu}_n$ in the eco-evo model, resulting from the heritability of resistance or the fecundity cost of resistance, thus alter $\bar{\nu}_n$ in the SEIR model.

Because we have no information about the extent to which variation in risk changes between generations, we again assume that the coefficient of variation C is constant. The eco-evo model therefore tracks changes in average risk $\bar{\nu}_n$ only. Because C describes variation in the overall distribution of risk, it represents a combination of environmental and genetic variation. The term bC^2 then represents genetic variation, specifically the squared coefficient of variation of the genotypic distribution, so b is the (narrow-sense) heritability.

The most complex trade-off model that could be supported by Páez et al.'s (2017) experimental data was linear; we therefore assume that fecundity increases linearly with infection risk, with baseline fecundity r_n and with slope $r_n s$. To understand the effect of this assumption on the model, recall that the average risk at time t during the epizootic is $\bar{\nu}(S(t)/S(0))^{C^2}$. At the end of the epizootic, when $t = T$, the cumulative fraction infected is $i(N_n, Z_n, \bar{\nu}_n) \equiv 1 - S(T)/S(0)$. It follows that the average risk at the end of the epizootic is $\bar{\nu}[1 - i(N_n, Z_n, \bar{\nu}_n)]^{C^2}$. Summing per capita fecundity across individuals with different infection risk is then equivalent to averaging risk across individuals, so per capita fecundity is $r_n + r_n s\bar{\nu}_n[1 - i(N_n, Z_n, \bar{\nu}_n)]^{C^2}$ (Páez et al. 2017). The expression for the effect of the trade-off on average infection risk results from a similar derivation. Changes in the densities of the host and the pathogen and in average infection risk are thus driven not just by ecological mechanisms but also by balancing selection for host resistance and host fecundity.

Increased host variation acts both to lower epizootic severity and to increase the rate of evolutionary change; because of these countervailing effects, the eco-evo model can show sustained cycles even if variation $C > 1$ and even if stochasticity $\sigma_L = 0$ (Páez et al. 2017). To ensure a fair comparison between models, however, we included stochasticity in the eco-evo model by allowing baseline fecundity r_n to change randomly in each generation, as in the eco-only model. Deterministic versions of the eco-evo model nevertheless fit the data better than stochastic versions, as we will show.

Fitting Models to Data

Because the baculovirus epizootic data and the *L. dispar* outbreak data were collected independently of each other, we fitted our models separately to the two types of data. This in turn meant that we were able to take advantage of

the nesting of the SEIR model inside the long-term models by carrying out the model fitting in two steps (fig. 1). In step 1, we fitted the SEIR model to data from baculovirus epizootics and experiments. The epizootic data provide weekly estimates of the fraction of larvae dying over single larval seasons in multiple populations (Woods and Elkinton 1987). The experimental data provide estimates of baculovirus transmission rates from single branches in the field and estimates of speeds of kill from cups in the laboratory (Elderd et al. 2008; Fleming-Davies et al. 2015; Páez et al. 2017).

In step 2, we fitted the long-term models to the handful of published time series of *L. dispar* densities that include more than one outbreak (appendix). Because these data include no information about the baculovirus, we used the parameters of the within-season SEIR models from step 1 as parameters for the within-season SEIR models nested in the long-term models in step 2. The parameter estimates from step 1 thus made up for the lack of information about the baculovirus in the long-term data. The baculovirus epizootic data and the *L. dispar* outbreak data were collected over very different timescales: 6–10 weeks for the epizootic data and 11–17 years for the outbreak data (spatial scales were similar: 4–9 ha for the epizootic data, 1.5–18 ha for the outbreak data). By using the SEIR model parameters from step 1 as parameters in the long-term models in step 2, we were thus using data collected over short temporal scales to explain data collected over long temporal scales.

The epizootic data and the experimental data were correspondingly collected over very different spatial scales: on branches that included ≈1 m^2 of foliage for the experimental data and in 4–9-ha forest plots for the epizootic data (temporal scales were similar: 1–3 weeks for experiments, 6–10 weeks for epizootics). By using the experimental data to estimate the within-season SEIR model parameters in step 1, we were therefore using data collected at small spatial scales to help explain data collected at large spatial scales. Across the two steps in our model fitting, we thus tested the extent to which small-scale data can explain large-scale data. These tests were important because they provided a way of testing the prediction of eco-evo theory that natural selection at the scale of an individual can explain host-pathogen dynamics at the scale of a population.

We thus followed a long-standing approach to model testing in ecology in which small-scale data are used to estimate model parameters and to generate model predictions and large-scale data are used to test the model predictions (Kareiva and Odell 1987; Keeling et al. 2001; Halloran et al. 2002; George et al. 2011; Blackwood et al.

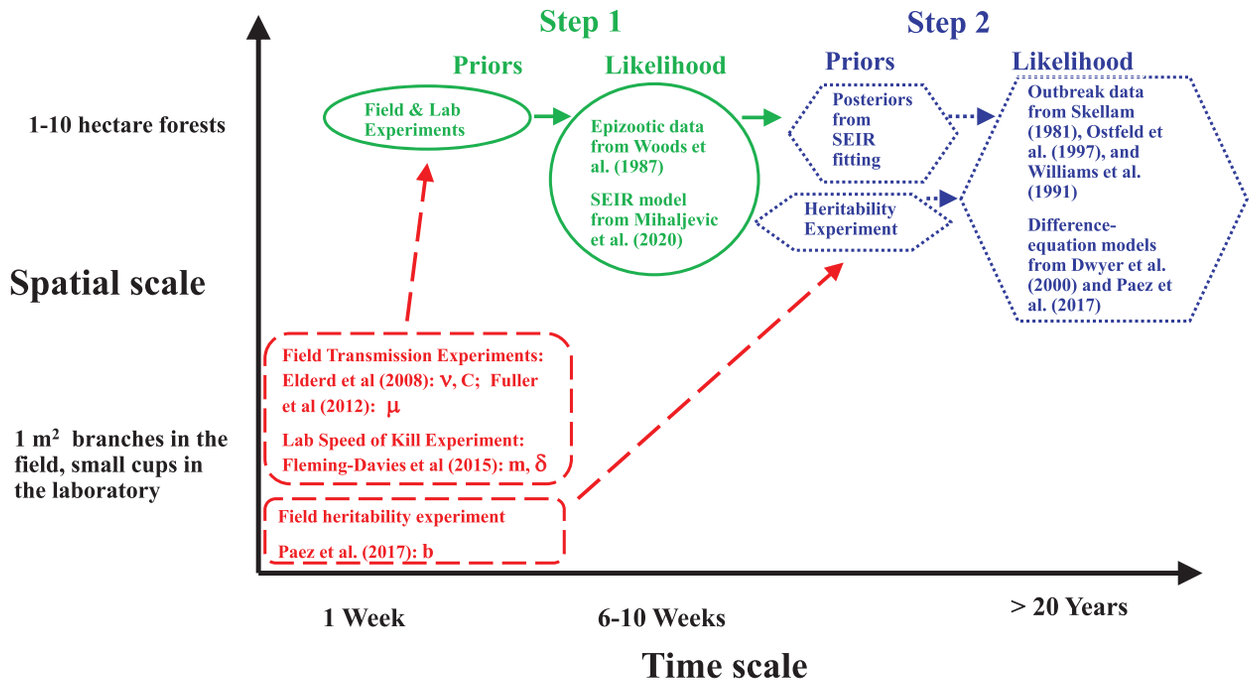

Figure 1: Overview of model fitting. Red dashed rectangles and arrows indicate experimental data, green solid circles and lines indicate priors and likelihoods of susceptible-exposed-infectious-removed (SEIR) models fitted to baculovirus epizootic data, and blue dotted hexagons and lines indicate priors and likelihoods of long-term models fitted to *Lymantria dispar* outbreak data.

2013; Searle et al. 2016). Most applications of this approach, however, have used only point estimates of the model parameters and only qualitative comparisons of model predictions to large-scale data. Using point estimates of the model parameters is problematic because the nonlinearities that are inherent in most ecological models can turn a small amount of uncertainty in a model's parameters into a large amount of uncertainty in a model's predictions (Elderd et al. 2006). Using qualitative comparisons of models to data is problematic because qualitative comparisons can conceal biologically meaningful differences in the fit of different models (Hunter and Dwyer 1998); as we described in the introduction, this latter problem is likely part of the reason why eco-evo theory has had a limited impact on ecology.

In testing whether small-scale data can explain large-scale data, we therefore allowed for parameter uncertainty, and we compared models to data on the basis of quantitative criteria. To do this, we generated model predictions for distributions of model parameters rather than for point estimates of model parameters, and we calculated likelihood scores rather than relying on visual comparisons of models to data. To carry out this procedure in a statistically robust way, we used Bayesian statistical techniques; this means that we constructed prior distributions from small-scale data, and we combined the priors with likelihoods from large-scale data to form posterior distributions of the model parameters (Gelman et al. 2014). We then used the posterior distributions of the parameters to calculate WAIC model selection scores, and we used the WAIC scores to choose between models.

Like the non-Bayesian AIC (Burnham and Anderson 2002), WAIC balances the better fit of more complex models against the greater parsimony of simpler models (Gelman et al. 2014). To do this, WAIC assigns each model a goodness-of-fit score, which is equal to twice the model's negative log likelihood averaged across the posterior distribution of the model parameters, and a penalty score, which is equal to the variance in the model's log likelihood calculated across the posterior distribution of the model parameters (appendix). WAIC assigns smaller (better) negative average log likelihoods to better-fitting models, which often have more parameters, but it assigns higher penalty scores to models with more variable predictions, which are often produced by models that have more parameters. Following a rule of thumb from the theory of model selection (Burnham and Anderson 2002), we conclude that one model fits the data better than a second model if the first model's WAIC score is at least 3 points better (lower) than the WAIC score for the second model; otherwise, we conclude that the fits of the two models are statistically indistinguishable (Bolker 2008).

In step 1 of our model fitting, WAIC allowed us to compare cases in which we used experimental data to construct priors (appendix) to cases in which we used uninformative or "vague" priors, which assign equal probability to large parameter ranges and therefore include no information from the experimental data. (Following statistical practice, we refer to cases with different priors as different models even when the underlying mathematical models are the same.) We then compare WAIC scores for the models with experiment-based priors to WAIC scores for the models with vague priors. Meaningfully better WAIC scores for the models with experiment-based priors then indicate that the small-scale experimental data improve our inferences about the large-scale epizootic data and thus that the small-scale data help explain the large-scale data (Mihaljevic et al. 2020).

In both steps in our model fitting, the two best models included a model that had vague priors and a model that had experiment-based priors, and in both steps the two best models had statistically indistinguishable WAIC scores. Because of the differences in priors, however, in both steps the two best models had different posterior means for at least one parameter, indicating that the models provide biologically different explanations for the data. Because experiments can provide deeper insights into underlying mechanisms than model fitting alone, in both cases we conclude that the model with experiment-based priors is the best model. We therefore further conclude that the small-scale data, in the form of experiment-based priors, help to explain the large-scale data.

In step 2, we followed Kendall et al. (1999) in fitting the long-term models only to the periods and amplitudes of the *L. dispar* time series rather than to the entirety of each time series. Fitting the entirety of a time series would likely have required that we know the initial value of the pathogen density as well as the initial value of infection risk for the eco-evo models, but both are unknown. Long-term model periods and amplitudes are in contrast independent of the initial values of the state variables (Rasband 2015), so fitting the models to the periods and amplitudes did not require initial values of pathogen density or infection risk. Fitting the models to periods and amplitudes further allowed us to avoid fitting the average infection risk $\bar{\nu}$ in the eco-only model and the relative slope parameter s in the eco-evo model (appendix), because those parameters affect only the equilibrium values of the state variables.

These details are important because fitting the models to the average period and average amplitude meant that adding stochasticity did not improve the fit of the eco-evo models to the data. This is because in models like the eco-evo models that show sustained cycles without stochasticity, stochasticity mostly changes the variance of the cycle period rather than the average period (Dwyer et al. 2004). Meanwhile, none of the *L. dispar* outbreak time series spanned more than two outbreaks, so we were not able to estimate the variance in the period from the data, which in turn

meant that we were not able to include the variance in the period as one of the statistics to which we fitted the models. Stochasticity therefore had little effect on the fit of the eco-evo models to the data. For the eco-only models, in contrast, stochasticity is necessary for the models to produce realistic cycles, as we will show.

The lack of an effect of stochasticity on the fit of the eco-evo models became clear in the first step in our model-fitting algorithm. The model-fitting algorithm combines an initial line-search step with a subsequent Metropolis-Hastings Markov chain Monte Carlo (MCMC) step and is therefore known as line-search MCMC (Kennedy et al. 2014). After the line-search step in the algorithm, a diagnostic can be generated by plotting marginal histograms of the parameters. In the case of the eco-evo models, the marginal histograms for the stochasticity parameters were almost flat for stochasticity values near zero; indeed, zero stochasticity gave the highest values of the posteriors, but values that were slightly larger were nearly as good. It therefore appears that the eco-evo models without stochasticity provide the best fit to the data; we were unable to use WAIC to conclusively demonstrate this better fit, however, because the MCMC algorithm in step 2 of our model fitting did not converge for the stochastic eco-evo models, likely because of the flatness of the marginal posteriors for the stochasticity parameter. Although it may therefore be true that for the eco-evo models there is some low, nonzero value of stochasticity that allows for an even better fit than zero stochasticity, our main goal was to compare the eco-evo models and the eco-only models; accordingly, the possible existence of a nonzero value of stochasticity that gives a better fit of the eco-evo models to the data is of little interest. More broadly, although stochasticity likely affects *L. dispar* outbreak cycles in nature, the flatness of the marginal histograms on the stochasticity parameter makes clear that adding stochasticity to the eco-evo models would not have changed our conclusions. Generalist predators similarly affect mostly the variance in the period (Dwyer et al. 2004), so we did not include generalist predators either.

A related point is that in step 2 we did not use time-series data of the area defoliated by *L. dispar* (Johnson et al. 2005; Bjornstad et al. 2010), even though such time series are often longer than the available time series of *L. dispar* densities. The problem is that the area-defoliated data do not have a clear relationship to *L. dispar* larval density; area defoliated data therefore can be used to calculate the period of *L. dispar* outbreak cycles but not the amplitude. If we had fitted our models to area-defoliated data, we would therefore have run a high risk that the best models would show damped cycles with the correct period but with an unrealistically small amplitude, biasing our fitting procedure against the eco-evo models. Reassuringly, periods in area-defoliated data range from 8 to 12 years (Johnson et al. 2005) and are thus reasonably close to the 9–12-year range in the density data.

Results

Eco-Evo Models Better Explain the Lymantria dispar Outbreak Data

In step 1, the best SEIR model ("SEIR + Transm'n") has experiment-based priors on the average transmission parameter $\bar{\nu}$ and on the inverse host variation parameter $k = 1/C^2$, while the second-best model ("SEIR + All") has experiment-based priors on all biologically meaningful parameters, meaning all but the stochasticity and measurement error parameters (fig. 2). The WAIC score for the second-best model is less than 3 points higher than the score for the best model ($\Delta\text{WAIC} < 3$), however, so the fits of the two models are statistically indistinguishable (Bolker 2008). In contrast, for the third-best model, which has experiment-based priors on the death rate δ and on the number of exposed classes m, the WAIC difference (ΔWAIC) is more than 5. This value is sufficiently large that we do not show a visual comparison of this model's predictions to data, and we did not use the model's posterior as a prior in step 2.

The two best SEIR models are able to explain most of the epizootic data. Both models underestimate the late-season infection rate in one population (initial density: 32 larvae/m^2), while the second-best model underestimates the infection rate in a second population (initial density: 9 larvae/m^2). These discrepancies are relatively modest, however, so for the best model $r^2 = 0.57$, while for the second-best model $r^2 = 0.70$ (fig. 2; because of the difference in how likelihoods and r^2 values are calculated and because of the small ΔWAIC score for the two best models, we do not expect agreement between WAIC scores and r^2 values; see the appendix for an explanation of how we calculated r^2). Our results from step 1 thus suggested that the posteriors from the two best epizootic models could help us make inferences about the long-term models in step 2.

Our results from step 2 then show that the best long-term model is the eco-evo model that uses an experiment-based prior on heritability b and that uses priors based on the SEIR + All model (step 2: "Eco-evo + experimental b/SEIR + All model"; fig. 2). The second-best model is the eco-evo model that uses a vague prior on b but that also uses the SEIR + All model ("Eco-evo/SEIR + All model"). For the second-best model, the WAIC difference (ΔWAIC) is less than 2, again indicating that the explanations provided by the two best models are statistically indistinguishable. In contrast, the best eco-only model ("Eco-only/SEIR + All model") has a ΔWAIC of more than 8, a substantial difference. We therefore conclude that eco-evo models

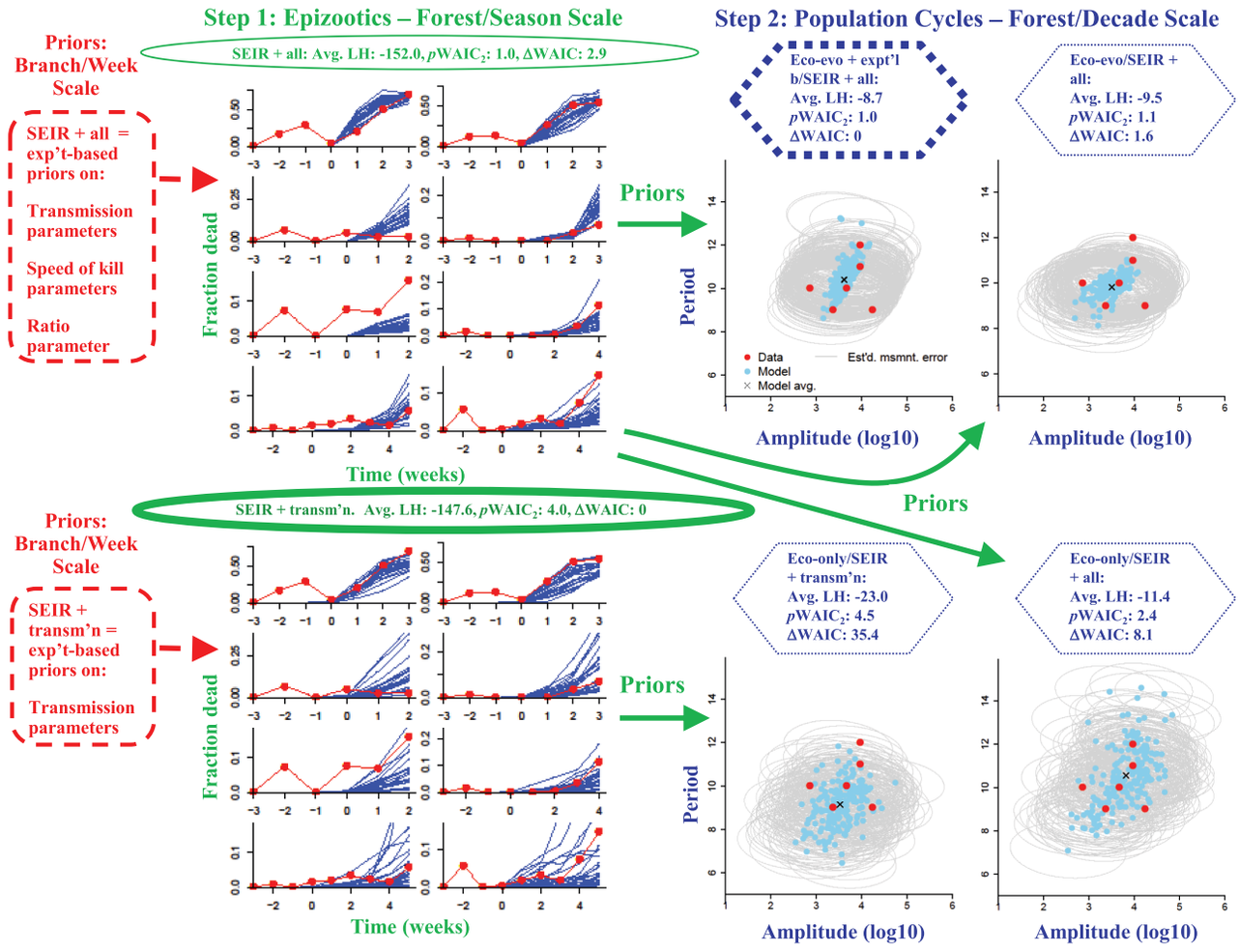

Figure 2: Model-fitting results. Following figure 1, red dashed rectangles and arrows indicate experiment-based priors on within-season susceptible-exposed-infectious-removed (SEIR) parameters, solid green ovals and arrows indicate Watanabe-Akaike information criterion (WAIC) analyses for within-season SEIR models, and dotted blue hexagons indicate WAIC analyses for the eco-evo and eco-only models. The WAIC score for the best model is indicated by a bold-lined oval in step 1 and by a bold-lined hexagon in step 2. "Avg. LH" refers to the log likelihood averaged across the posterior, $p\text{WAIC}_2$ indicates the penalty term, and ΔWAIC is the difference between a model's WAIC score and the best score. Under step 1, we compare SEIR model predictions with epizootic data, with the best model in the lower plot and the second best in the upper plot. Each subplot represents a distinct population with its own initial host and pathogen densities (Woods and Elkinton 1987). Subplots are arranged according to initial host density, with the highest density at the upper left, the second highest density at the upper right, and the lowest density at the lower right; following this ordering, the densities are 166, 62, 32, 24, 9, 7, 6, and 3 larvae/m^2. The blue lines in the subplots show 25 realizations of each model, and the red points show the data. Red points at negative times represent the fraction infected among hatchlings and therefore serve to determine the initial inputs of virus (appendix). We do not show results for the worst model, which has an average likelihood of −150.8, a penalty term ($p\text{WAIC}_2$) of 3.4, and a WAIC difference (ΔWAIC) of 5.1. Under step 2, the smaller sky-blue points show the model predictions for a large draw from the posterior of each model, and the larger red points show the data. The black cross symbols show the average model predictions, and the gray ovals show the estimated measurement error for each model prediction. Measurement error is shown in the form of tenth percentiles of normal distributions that use each predicted period-amplitude combination as means and error variances and error covariances calculated across the six data points. We do not show results for the worst model, which has an average likelihood of −34.8, a $p\text{WAIC}_2$ of 3.2, and a ΔWAIC of 56.3.

provide a much better explanation for *L. dispar* outbreak cycles than do eco-only models.

Figure 2 also shows the cycle periods and amplitudes in the models versus the cycle periods and amplitudes in the data. The two best eco-evo models must invoke measurement error to explain the data because for both models—and indeed for all of our long-term models—there is no single parameter set that can explain all six data points.

The amount of measurement error that the eco-evo models need to explain the data is further increased by data points that do not match the model predictions of the correlation between the cycle period and amplitude. Such correlations are typical of deterministic models that show sustained cycles (Rasband 2015), but as figure 2 shows not all of the data points match the predicted correlations for the two best models. Estimates of measurement errors are similarly high in empirical studies of *L. dispar* population cycles (Elkinton et al. 1996), however, suggesting that the model estimates of measurement error are consistent with field estimates of measurement error.

Meanwhile, the best eco-only model has a much worse WAIC score than the best eco-evo models. This is true even though the best eco-only model makes good predictions for many parameter sets (fig. 2); the problem is that for many other parameter sets, the model makes very poor predictions. Also, like the best eco-evo models, the best eco-only model must invoke high measurement error to explain the data. For the best eco-only model, however, the combination of high measurement error and a high frequency of poor predictions leads to a very poor log average likelihood and to very high variability in the log average likelihood.

The Importance of Experiment-Based Priors

The main reason why the eco-evo models provide a better explanation for the data than the eco-only models is that the within-season SEIR models nested in both sets of long-term models have priors that originated as posteriors for the best SEIR models. For the best within-season SEIR models, all of the posterior values of the inverse host variation parameter $k = 1/C^2 < 1$, while for the third-best SEIR model 48% of the posterior values of k are less than 1. These high levels of host variation are necessary for the SEIR models to explain how epizootic severity varies across host densities (Dwyer et al. 1997). Meanwhile, in the eco-evo models, which as we explained are deterministic, high host variation is consistent with realistic sustained cycles (fig. 3), but high host variation in deterministic versions of the eco-only models leads to unrealistic damped cycles. As we have seen, the eco-only models must then invoke high levels of stochasticity to explain the *L. dispar* outbreak

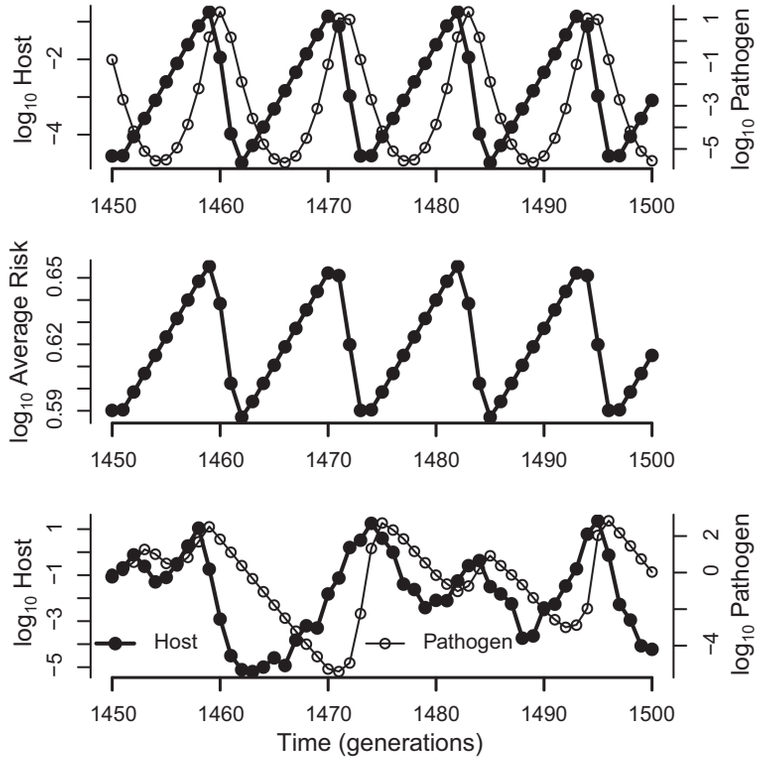

Figure 3: The top two panels show predictions of the eco-evo model, generated using the posterior median values of the parameters. The top panel shows host and pathogen densities, and the middle panel shows the average infection risk. The bottom panel shows a single realization of the best eco-only model, again generated using median posterior values of the parameters.

data, leading in turn to cycles with periods and amplitudes that are highly variable and far from the data (fig. 2). The eco-only models therefore have much worse WAIC scores.

Part of the reason why the posteriors of the within-season SEIR models are centered on high levels of host variation is that the SEIR models fitted to the epizootic data use priors that were constructed from experimental data (fig. 4), which in turn show high levels of host variation (Elderd et al. 2008). The experiment-based priors allowed the SEIR models to provide good fits to the epizootic data, which is why we used the posteriors of the SEIR models as priors for the long-term models. The experiment-based priors on k in particular indirectly explain the poor performance of the third-best SEIR model, which had a vague prior on k.

To explain this latter point we note first that for the SEIR models fitted to the epizootic data, the mean posterior values of $\bar{\nu}$ are extremely similar across models, while the posterior mean values of k for the two best models are only modestly lower than the posterior mean value of k for the third-best model (fig. 4). This is true even though the posterior means on k and $\bar{\nu}$ for the third-best model were determined entirely by the epizootic data, whereas the posterior means on k and $\bar{\nu}$ for the two best models were determined largely by the experimental data, as evidenced by the similarity of prior and posterior means for those models. Estimates of k and $\bar{\nu}$ from small-scale experiments are thus close to estimates of k and $\bar{\nu}$ from epizootics. The third-best model nevertheless has a worse WAIC score because its vague priors on k and $\bar{\nu}$ led to high uncertainty in those parameters, leading in turn to a high penalty score that outweighed the model's slightly higher average likelihood compared with the second-best model (fig. 2). Experiment-based priors on k and $\bar{\nu}$ therefore improved

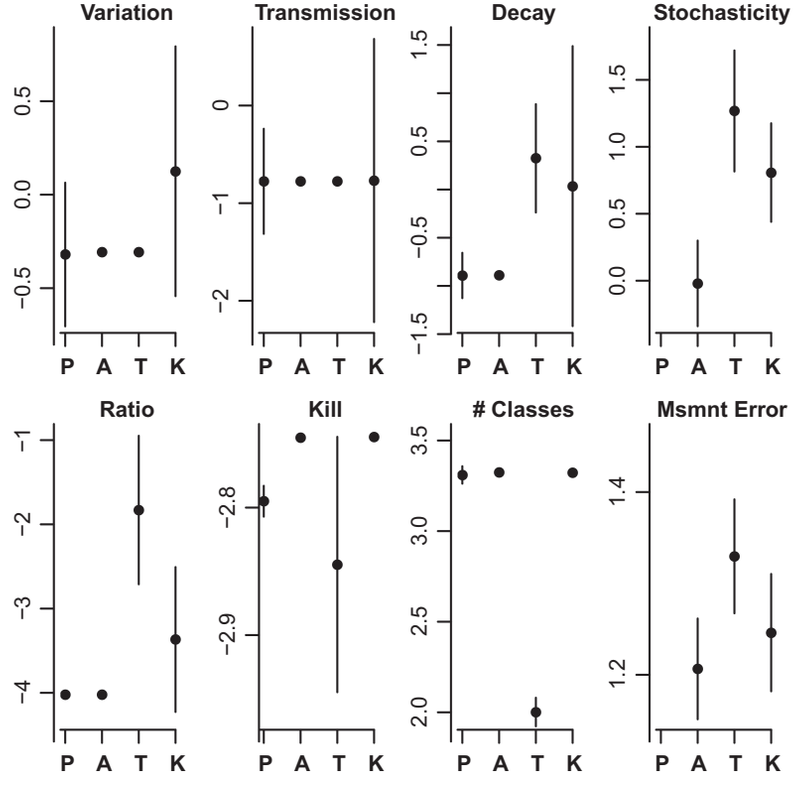

Figure 4: Comparison of parameter values across epizootic models. The label on each graph identifies the parameter being plotted, with points indicating means and vertical bars indicating 1 standard deviation, with both means and standard deviations calculated on a $\log_e$ scale. On the horizontal axes, "P" indicates the experiment-based priors themselves, "T" indicates the model with experiment-based priors on the transmission parameters $\bar{\nu}$ and C, "A" indicates the model with experiment-based priors on all biological parameters (not stochasticity or measurement error), and "K" indicates the model with experiment-based priors on the death rate parameter δ and the number of exposed classes m. "Variation" indicates the inverse host variation parameter $k = 1/C^2$, "Transmission" indicates the average transmission parameter/infection risk parameter $\bar{\nu}$ (units of m^2/day), "Decay" indicates the decay parameter μ (units of 1/day), "Stochasticity" indicates the stochasticity parameter σ_E, "Ratio" indicates the ratio parameter ρ (see the appendix), "Kill" indicates the death rate parameter δ (units of 1/day), "# Classes" indicates the number of exposed classes m, and "Msmnt Error" refers to the measurement error parameter η.

our inferences partly by reducing the uncertainty in our posterior estimates of k and $\bar{\nu}$.

The number of exposed classes m is a second parameter for which an experiment-based prior improved our inferences about the long-term models. The SEIR + All model, for which both the experiment-based prior and the posterior have mean $m = 27.8$, is used in the three best long-term models, including the two best eco-evo models and the best eco-only model. The two worst long-term models, in contrast, use the SEIR + Transm'n model, which has a vague prior and a posterior with mean $m = 7.40$ (fig. 2). The difference in posterior mean values of m between the SEIR + All model and the SEIR + Transm'n model is important because high values of m produce outbreak cycles with realistically long periods and large amplitudes, whereas small values of m produce outbreak cycles with unrealistically short periods and small amplitudes. Because the effects of m are due to a kind of stage structure in the exposed classes, the strong effect of m in our best models supports the general theoretical result that stage structure can help drive population cycles (Barraquand et al. 2017).

The observation that the posterior values of m for the best within-season SEIR model were much lower than for the second-best within-season SEIR model nevertheless raises the question, Has our reliance on the second-best SEIR model caused us to make incorrect inferences about *L. dispar* population cycles? To begin with, the small WAIC difference for the second-best SEIR model ($\Delta\text{WAIC} < 3$) makes clear that the fit of the second-best model is not much worse than the fit of the best model, while its lower penalty score means that the second-best model is more parsimonious. Moreover, as we mentioned earlier, in cases in which two models have similar WAIC scores but dissimilar posterior parameter distributions, it seems likely that the model with experiment-based parameters will better represent the underlying biology. Supporting this claim, the second-best model's high posterior mean on m is equivalent to assuming that there is only a vanishingly small probability of a speed of kill of less than 7 days or of more than 25 days (fig. 5), matching the experimental data both for the *L. dispar* baculovirus (Fleming-Davies et al. 2015) and for other insect baculoviruses (Cory and Myers 2003). The low posterior mean on m in the best model, in contrast, means that for that model speeds of kill of less than 5 days or more than 30 days are not unlikely (fig. 5), whereas such extreme speeds of kill are essentially never observed in experiments. We therefore argue that the better fit of the eco-evo models relative to the eco-only models is indeed based on robust inferences about the within-season SEIR models.

The heritability parameter b provides a final case in which an experiment-based prior improved our inferences about *L. dispar* outbreaks. Because the two best eco-evo models have statistically indistinguishable WAIC scores ($\Delta\text{WAIC} < 2$), we again argue that the model with an experiment-based prior is the best model; in this case, the model with an experiment-based prior also has the best WAIC score. Because the heritability experiment was carried out at the scale of a single branch while the outbreak data were collected at the scale of entire forest plots, the best model thus shows that a branch-scale mechanism can drive forest-scale outbreaks. Notably, however, the posterior mean value of b for the best model falls between its experiment-based prior mean and the posterior mean for the second-best model (fig. 6), emphasizing the importance of allowing for both experimental and observational data.

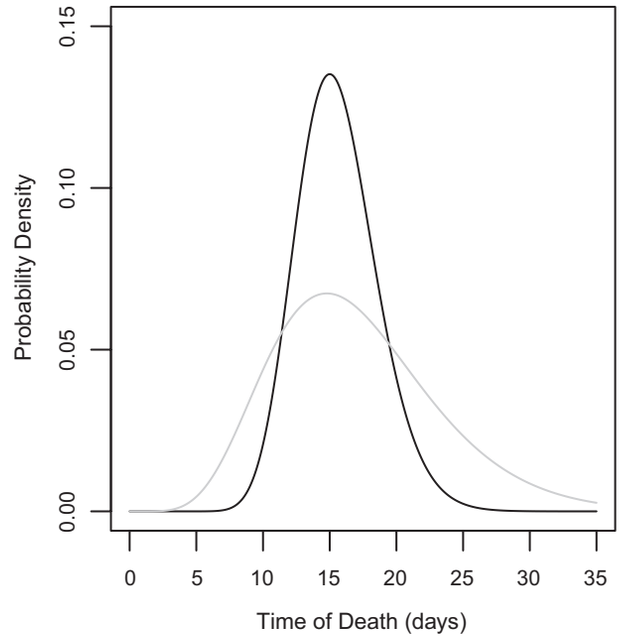

Figure 5: Distributions of times to death for two different versions of the susceptible-exposed-infectious-removed (SEIR) model, each using posterior mean values of the death rate parameter δ and the number of exposed classes m. Black indicates the version of the model for which all biological priors have experiment-based priors, while gray indicates the version with vague priors on δ and m.

Discussion

Our main result is that an eco-evo model does a better job of explaining *Lymantria dispar* population cycles than does an eco-only model (fig. 2). We therefore conclude that eco-evo theory can indeed explain population cycles in the field. Our work thus provides the kind of supporting example

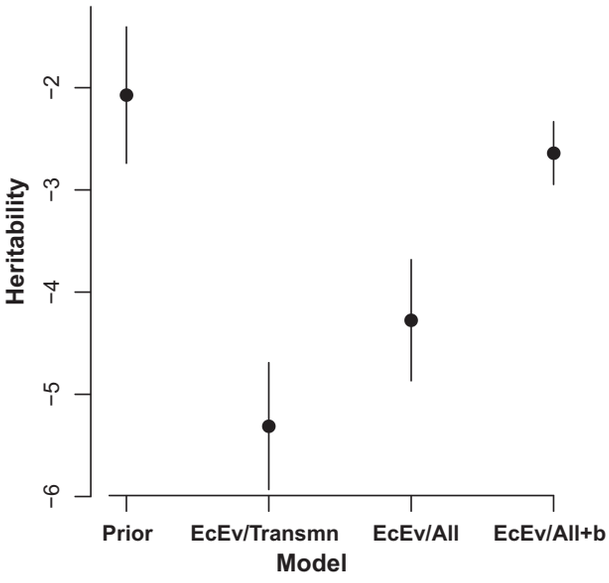

Figure 6: Means and standard deviations of prior and posterior means on $\log_e$ heritability for different versions of the eco-evo models. Here, "Prior" indicates the experiment-based prior, while the remaining abbreviations refer to the models in figure 2: "EcEv/Transmn" indicates the Eco-evo/SEIR + Transm'n model, "EcEv/All" indicates the Eco-evo/SEIR + All model, and "EcEv/All+b" indicates the Eco-evo/SEIR + All + *b* model.

that Hendry (2019) argued is needed for eco-evo theory to be viewed as a success.

Baculovirus-driven cycles in western tent caterpillars (Cory and Myers 2009) and nematode-driven cycles in red grouse (Martinez-Padilla et al. 2019) and Soay sheep (Hayward et al. 2019) have similarly been suggested to represent examples of eco-evo consumer-resource cycles. Eco-evo cycles may therefore be common in nature. Previous work, however, has relied on small-scale experiments alone. We hope to have instead demonstrated the importance of using large-scale observational field data to test eco-evo theory. We thus follow the ecological literature in arguing for the primacy of observational field data (Carpenter 1996); it is also true, however, that the incompleteness of the observational field data for *L. dispar* means that the support that the *L. dispar* data provide for eco-evo insect outbreak models is weaker than the support that laboratory data provide for eco-evo microcosm models (Yoshida et al. 2003; Hiltunen et al. 2014).

Our focus on field data nevertheless allowed us to show that the out-of-phase cycles seen in experimental microcosm studies do not necessarily occur in nature; in contrast to the half-cycle-period lags that occur in eco-evo microcosm models, the lags in our eco-evo models never exceed a single generation within a cycle period of 8–12 years (fig. 3). Support for this model prediction comes from observations of baculovirus infection rates. In both *L. dispar* (Woods and Elkinton 1987) and other forest defoliators (Moreau and Lucarotti 2007), infection rates peak in the year following the peak in the insect population.

Why do microcosm models show out-of-phase cycles while our models do not? A definitive answer to this question is beyond the scope of our work, but a key difference is that our models use difference equations to describe the seasonal conditions typical of the field whereas microcosm models use differential equations to describe the constant conditions typical of the laboratory (Cortez and Ellner 2010; Ellner 2013). Given that the vast majority of host-pathogen interactions are affected by seasonality (Altizer et al. 2006; Filion et al. 2020; Poulin 2020), we argue that difference equations provide a more realistic description of the dynamics of host-pathogen interactions in nature. This is important because the high frequency with which out-of-phase cycles occur in microcosms has been used to argue that eco-evo dynamics can be detected through visual inspection of consumer-resource time-series data (Hiltunen et al. 2014). Our results instead suggest that detecting eco-evo dynamics may require more complex analyses.

Because WAIC scores for models with experiment-based priors were close to or better than WAIC scores for models with vague priors, our inferences were strengthened by our use of experiment-based priors. We therefore argue that mechanisms operating in small-scale baculovirus field experiments can help to explain large-scale baculovirus epizootics and *L. dispar* outbreak cycles. Branch-scale transmission thus supplies a mechanism by which individual-scale natural selection can help drive population-scale consumer-resource cycles, supporting a fundamental prediction of eco-evo theory.

In addition to emphasizing eco-evo dynamics, our results also show that low variation in the speed of kill, which is equivalent to the incubation time in models of nonfatal diseases, plays an important role in driving insect outbreak cycles. Similar incubation-time effects have been inferred from time-series data on childhood diseases (Black et al. 2009), but to our knowledge the only evidence for incubation-time effects in animal diseases is based on small-scale experimental data alone (Peace et al. 2019). Our work thus provides rare evidence for effects of incubation-time delays on host-pathogen cycles in the field.

The importance of both incubation-time delays and natural selection in our results illustrates the fundamental principle that any ecological phenomenon is likely to be the result of multiple mechanisms (Quinn and Dunham 1983). Indeed, high host variation is also consistent with realistic insect outbreak cycles in models with multiple pathogen strains (Fleming-Davies et al. 2015) and in models with

changes in insect-host variation that result from defoliation-driven increases in host-plant defenses (Elderd et al. 2013). Because previous work relied on qualitative comparisons of models to data, the evidence for our eco-evo models is stronger than it is for alternative models, but the experimental evidence in favor of alternative models is nevertheless quite strong. It therefore seems likely that *L. dispar* population cycles are also affected by induced plant defenses and by the occurrence of phenotypic variation in baculovirus strains.

As we mentioned, since 1989 *L. dispar* outbreaks have usually been terminated by *Entomophaga maimaiga* (Kyle et al. 2020), but in a recent outbreak baculovirus infection rates were apparently almost as high as *E. maimaiga* infection rates (Elkinton et al. 2019). Climate change may thus be reducing the competitive ability of the weather-sensitive *E. maimaiga*, allowing the baculovirus to again play a key role in terminating *L. dispar* outbreaks. Meanwhile, artificial control of *L. dispar* outbreaks is usually accomplished using the bacterial toxin Btk, which is far cheaper than the baculovirus spray product Gypchek (Podgwaite et al. 1992; Webb et al. 2005) but which kills Lepidoptera indiscriminately (Hajek and Tobin 2010). Public pressure has therefore led to increased use of Gypchek (*Circleville Herald* 2020). This increased use is important for our work because eco-only models have shown that repeated applications of Gypchek may damp out outbreak cycles (Reilly and Elderd 2014), whereas the destabilizing effect of eco-evo dynamics in our models suggests that eco-evo dynamics may prevent repeated Gypcheck applications from damping out outbreak cycles (Páez and Fleming-Davies 2020). Extending our eco-evo models to understand the consequences of baculovirus spraying is therefore an important direction for future research.

Acknowledgments

G.D. and V.D. were supported by National Institutes of Health grant R01GM96655, awarded to G.D., V.D., and B. J. Rehill. Research was conducted under US Department of Agriculture Animal and Plant Health Inspection Service permit P526P-12-01466 to G.D. G.D. was supported by National Science Foundation grant OPUS DEB-2043796. Bret Elderd provided data from his experiments in the early 2000s.

Statement of Authorship

G.D. conceived of the project, wrote the code, and wrote most of the text. J.R.M. provided extremely useful edits to the text and had useful discussions with G.D. At crucial moments, V.D. prevented G.D. from making statistical errors.

Data and Code Availability

The code is available in G.D.'s GitHub repository (https://github.com/gregvirus2/EcoEvoModelDwyerEtAl2021AmNat) and on Zenodo (https://doi.org/10.5281/zenodo.4625661).

Literature Cited

Altizer, S., A. Dobson, P. Hosseini, P. Hudson, M. Pascual, and P. Rohani. 2006. Seasonality and the dynamics of infectious diseases. Ecology Letters 9:467–484.

Anderson, R. M., and R. M. May. 1980. Infectious diseases and population cycles of forest insects. Science 210:658–661.

———. 1992. Infectious diseases of humans: dynamics and control. Oxford University Press, Oxford.

Barraquand, F., S. Louca, K. C. Abbott, C. A. Cobbold, F. Cordoleani, D. L. DeAngelis, B. D. Elderd, et al. 2017. Moving forward in circles: challenges and opportunities in modelling population cycles. Ecology Letters 20:1074–1092.

Bjornstad, O. N., R. Christelle, and A. M. Liebhold. 2010. Geographic variation in North American gypsy moth cycles: subharmonics, generalist predators, and spatial coupling. Ecology 91:106–118.

Black, A. J., A. J. McKane, A. Nunes, and A. Parisi. 2009. Stochastic fluctuations in the susceptible-infective-recovered model with distributed infectious periods. Physical Review E 80:021922.

Blackwood, J. C., D. G. Streicker, S. Altizer, and P. Rohani. 2013. Resolving the roles of immunity, pathogenesis, and immigration for rabies persistence in vampire bats. Proceedings of the National Academy of Sciences of the USA 110:20837–20842.

Bolker, B. M. 2008. Ecological models and data in R. Princeton University Press, Princeton, NJ.

Briggs, C., and H. Godfray. 1996. The dynamics of insect-pathogen interactions in seasonal environments. Theoretical Population Biology 50:149–177.

Bruijning, M., E. Jongejans, and M. M. Turcotte. 2019. Demographic responses underlying eco-evolutionary dynamics as revealed with inverse modelling. Journal of Animal Ecology 88:768–779.

Burnham, K., and D. Anderson. 2002. Model selection and multimodel inference: a practical information-theoretic approach. Springer, New York.

Carpenter, S. R. 1996. Microcosm experiments have limited relevance for community and ecosystem ecology. Ecology 77:677–680.

Circleville Herald. 2020. Gypsy moth spraying to begin soon. Ohio, May 4.

Cobbold, C. A., J. Roland, and M. A. Lewis. 2009. The impact of parasitoid emergence time on host-parasitoid population dynamics. Theoretical Population Biology 75:201–215.

Cortez, M. H., and S. P. Ellner. 2010. Understanding rapid evolution in predator-prey interactions using the theory of fast-slow dynamical systems. American Naturalist 176:E109–E127.

Cortez, M. H., S. Patel, and S. J. Schreiber. 2020. Destabilizing evolutionary and eco-evolutionary feedbacks drive empirical eco-evolutionary cycles. Proceedings of the Royal Society B 287:20192298.

Cory, J. S., and J. H. Myers. 2003. The ecology and evolution of insect baculoviruses. Annual Reviews of Ecology and Systematics 34:239–272.

———. 2009. Within and between population variation in disease resistance in cyclic populations of western tent caterpillars: a test of the disease defence hypothesis. Journal of Animal Ecology 78:646–655.

Diss, A., J. Kunkel, M. Montgomery, and D. Leonard. 1996. Effects of maternal nutrition and egg provisioning on parameters of larval hatch, survival and dispersal in the gypsy moth, *Lymantria dispar* L. Oecologia 106:470–477.

Duffy, M. A., J. H. Ochs, R. M. Penczykowski, D. J. Civitello, C. A. Klausmeier, and S. R. Hall. 2012. Ecological context influences epidemic size and parasite-driven evolution. Science 335:1636–1638.

Duffy, M. A., and L. Sivars-Becker. 2007. Rapid evolution and ecological host-parasite dynamics. Ecology Letters 10:44–53.

Dwyer, G., J. Dushoff, J. S. Elkinton, and S. A. Levin. 2000. Pathogen-driven outbreaks in forest defoliators revisited: building models from experimental data. American Naturalist 156:105–120.

Dwyer, G., J. Dushoff, and S. H. Yee. 2004. The combined effects of pathogens and predators on insect outbreaks. Nature 430:341–345.

Dwyer, G., and J. S. Elkinton. 1993. Using simple models to predict virus epizootics in gypsy-moth populations. Journal of Animal Ecology 62:1–11.

Dwyer, G., J. S. Elkinton, and J. P. Buonaccorsi. 1997. Host heterogeneity in susceptibility and disease dynamics: tests of a mathematical model. American Naturalist 150:685–707.

Elderd, B. D., V. M. Dukic, and G. Dwyer. 2006. Uncertainty in predictions of disease spread and public-health responses to bioterrorism and emerging diseases. Proceedings of the National Academy of Sciences of the USA 103:15693–15697.

Elderd, B. D., J. Dushoff, and G. Dwyer. 2008. Host-pathogen interactions, insect outbreaks, and natural selection for disease resistance. American Naturalist 172:829–842.

Elderd, B. D., B. J. Rehill, K. J. Haynes, and G. Dwyer. 2013. Induced plant defenses, host-pathogen interactions, and forest insect outbreaks. Proceedings of the National Academy of Sciences of the USA 110:14978–14983.

Elkinton, J. S., T. D. Bittner, V. J. Pasquarella, G. H. Boettner, A. M. Liebhold, J. R. Gould, H. Faubert, et al. 2019. Relating aerial deposition of *Entomophaga maimaiga* conidia (Zoopagomycota: Entomophthorales) to mortality of gypsy moth (Lepidoptera: Erebidae) larvae and nearby defoliation. Environmental Entomology 48:1214–1222.

Elkinton, J. S., W. M. Healy, J. Buonaccorsi, G. H. Boettner, and A. M. Hazzard. 1996. Interactions among gypsy moths, white-footed mice, and acorns. Ecology 77:2332–2342.

Ellner, S. P. 2013. Rapid evolution: from genes to communities, and back again? Functional Ecology 27:1087–1099.

Elton, C. S. 1924. Periodic fluctuations in the numbers of animals: their causes and effects. Journal of Experimental Biology 2:119–163.

Filion, A., A. Eriksson, F. Jorge, C. N. Niebuhr, and R. Poulin. 2020. Large-scale disease patterns explained by climatic seasonality and host traits. Oecologia 194:723–733.

Fleming-Davies, A. E., V. Dukic, V. Andreasen, and G. Dwyer. 2015. Effects of host heterogeneity on pathogen diversity and evolution. Ecology Letters 18:1252–1261.

Fleming-Davies, A. E., and G. Dwyer. 2015. Phenotypic variation in overwinter environmental transmission of a baculovirus and the cost of virulence. American Naturalist 186:797–806.

Fuller, E., B. D. Elderd, and G. Dwyer. 2012. Pathogen persistence in the environment and insect-baculovirus interactions: disease-density thresholds, epidemic burnout, and insect outbreaks. American Naturalist 179:E70–E96.

Fuxa, J. R., and Y. Tanada. 1987. Epizootiology of insect diseases. Wiley, Hoboken, NJ.

Gelman, A., J. B. Carlin, H. S. Stern, D. B. Dunson, A. Vehtari, and D. B. Rubin. 2014. Bayesian data analysis. 3rd ed. Chapman & Hall/CRC Press, New York.

George, D. B., C. T. Webb, M. L. Farnsworth, T. J. O'Shea, R. A. Bowen, D. L. Smith, T. R. Stanley, L. E. Ellison, and C. E. Rupprecht. 2011. Host and viral ecology determine bat rabies seasonality and maintenance. Proceedings of the National Academy of Sciences of the USA 108:10208–10213.

Govaert, L., E. A. Fronhofer, S. Lion, C. Eizaguirre, D. Bonte, M. Egas, A. P. Hendry, et al. 2019. Eco-evolutionary feedbacks—theoretical models and perspectives. Functional Ecology 33:13–30.

Hajek, A. E., and P. C. Tobin. 2010. Micro-managing arthropod invasions: eradication and control of invasive arthropods with microbes. Biological Invasions 12:2895–2912.

Halloran, M. E., I. M. Longini, A. Nizam, and Y. Yang. 2002. Containing bioterrorist smallpox. Science 298:1428–1432.

Hanski, I. A. 2011. Eco-evolutionary spatial dynamics in the Glanville fritillary butterfly. Proceedings of the National Academy of Sciences of the USA 108:14397–14404.

Hassell, M., R. May, S. Pacala, and P. Chesson. 1991. The persistence of host-parasitoid associations in patchy environments. I. A general criterion. American Naturalist 138:568–583.

Hayward, A. D., R. Garnier, D. Z. Childs, B. T. Grenfell, K. A. Watt, J. G. Pilkington, J. M. Pemberton, and A. L. Graham. 2019. From population to individual host scale and back again: testing theories of infection and defence in the Soay sheep of St Kilda. Pages 91–128 *in* K. Wilson, A. Fenton, and D. Tompkins, eds. Wildlife disease ecology: linking theory to data and application. Cambridge University Press, Cambridge.

Hendry, A. P. 2019. A critique for eco-evolutionary dynamics. Functional Ecology 33:84–94.

Hiltunen, T., N. G. Hairston Jr., G. Hooker, L. E. Jones, and S. P. Ellner. 2014. A newly discovered role of evolution in previously published consumer-resource dynamics. Ecology Letters 17:915–923.

Hunter, A. F. 1995. Ecology, life history and phylogeny of outbreak and nonoutbreak species. Pages 41–64 *in* N. Cappuccino and P. Price, eds. Population dynamics: new approaches and synthesis. Academic Press, New York.

Hunter, A. F., and G. Dwyer. 1998. Outbreaks and interacting factors: insect population explosions synthesized and dissected. Integrative Biology 1:166–177.

Johns, R., L. Flaherty, D. Carleton, S. Edwards, A. Morrison, and E. Owens. 2016. Population studies of tree-defoliating insects in Canada: a century in review. Canadian Entomologist 148:S58–S81.

Johnson, D. M., A. M. Liebhold, and O. N. Bjørnstad. 2005. Circumpolar variation in periodicity and synchrony among gypsy moth populations. Journal of Animal Ecology 74:882–892.

Kareiva, P., and G. Odell. 1987. Swarms of predators exhibit "prey-taxis" if individual predators use area-restricted search. American Naturalist 130:233–270.

Keeling, M. J., and P. Rohani. 2008. Modeling infectious diseases in humans and animals. Princeton University Press, Princeton, NJ.

Keeling, M. J., M. E. Woolhouse, D. J. Shaw, L. Matthews, M. Chase-Topping, D. T. Haydon, S. J. Cornell, J. Kappey, J. Wilesmith, and B. T. Grenfell. 2001. Dynamics of the 2001 UK foot and mouth

epidemic: stochastic dispersal in a heterogeneous landscape. Science 294:813–817.

Kendall, B. E., C. J. Briggs, W. W. Murdoch, P. Turchin, S. P. Ellner, R. M. Nisbet, and S. N. Wood. 1999. Why do populations cycle? a synthesis of statistical and mechanistic modeling approaches. Ecology 80:1789–1805.

Kennedy, D. A., V. Dukic, and G. Dwyer. 2014. Combining principal component analysis with parameter line-searches to improve the efficacy of Metropolis–Hastings MCMC. Environmental and Ecological Statistics 22:247–274.

———. 2014. Pathogen growth in insect hosts: inferring the importance of different mechanisms using stochastic models and response-time data. American Naturalist 184:407–423.

Kot, M. 2001. Elements of mathematical ecology. Cambridge, Cambridge University Press.

Krylova, O., and D. J. Earn. 2013. Effects of the infectious period distribution on predicted transitions in childhood disease dynamics. Journal of the Royal Society Interface 10:20130098.

Kyle, C. H., J. Liu, M. E. Gallagher, V. Dukic, and G. Dwyer. 2020. Stochasticity and infectious disease dynamics: density and weather effects on a fungal insect pathogen. American Naturalist 195:504–523.

Liebhold, A., and N. Kamata. 2000. Introduction—are population cycles and spatial synchrony a universal characteristic of forest insect populations? Population Ecology 42:205–209.

Luo, S., and K. Koelle. 2013. Navigating the devious course of evolution: the importance of mechanistic models for identifying eco-evolutionary dynamics in nature. American Naturalist 181:S58–S75.

Martinez-Padilla, J., M. Wenzel, F. Mougeot, L. Perez-Rodriguez, S. Piertney, and S. M. Redpath. 2019. Parasite-mediated selection in red grouse—consequences for population dynamics and mate choice. Pages 296–320 *in* K. Wilson, A. Fenton, and D. Tompkins, eds. Wildlife disease ecology: linking theory to data and application. Cambridge, Cambridge University Press.

Mihaljevic, J. R., C. M. Polivka, C. J. Mehmel, C. Li, V. Dukic, and G. Dwyer. 2020. An empirical test of the role of small-scale transmission in large-scale disease dynamics. American Naturalist 195:616–635.

Moreau, G., and C. J. Lucarotti. 2007. A brief review of the past use of baculoviruses for the management of eruptive forest defoliators and recent developments on a sawfly virus in Canada. Forestry Chronicle 83:105–112.

Moreau, G., D. P. Ostaff, É. Bauce, E. S. Eveleigh, C. J. Lucarotti, B. Morin, and D. T. Quiring. 2018. Interlacing roles of bottom-up, top-down, endogenous, and anthropogenic factors in population oscillations. Ecosphere 9:e02421.

Murray, K. D., and J. S. Elkinton. 1989. Environmental contamination of egg masses as a major component of transgenerational transmission of gypsy-moth nuclear polyhedrosis-virus (LdMNPV). Journal of Invertebrate Pathology 53:324–334.

———. 1990. Transmission of nuclear polyhedrosis-virus to gypsy-moth (Lepidoptera, Lymantriidae) eggs via contaminated substrates. Environmental Entomology 19:662–665.

Myers, J. H. 1988. Can a general hypothesis explain population cycles of forest lepidoptera? Advances in Ecological Research 18:179–242.

———. 2018. Population cycles: generalities, exceptions and remaining mysteries. Proceedings of the Royal Society B 285:20172841.

Nisbet, R. M., and W. S. C. Gurney. 2003. Modelling fluctuating populations. Wiley Interscience, Hoboken, NJ.

Ohlberger, J., Ø. Langangen, E. Edeline, E. M. Olsen, I. J. Winfield, J. M. Fletcher, J. B. James, N. C. Stenseth, and L. A. Vøllestad. 2011. Pathogen-induced rapid evolution in a vertebrate life-history trait. Proceedings of the Royal Society B 278:35–41.

Oli, M. K. 2019. Population cycles in voles and lemmings: state of the science and future directions. Mammal Review 49:226–239.

Ostfeld, R. S., C. G. Jones, and J. O. Wolff. 1996. Of mice and mast. BioScience 46:323–330.

Páez, D. J., V. Dukic, J. Dushoff, A. Fleming-Davies, and G. Dwyer. 2017. Eco-evolutionary theory and insect outbreaks. American Naturalist 189:616–629.

Páez, D. J., and A. E. Fleming-Davies. 2020. Understanding the evolutionary ecology of host–pathogen interactions provides insights into the outcomes of insect pest biocontrol. Viruses 12:141.

Peace, A., S. M. O'Regan, J. A. Spatz, P. N. Reilly, R. D. Hill, E. D. Carter, R. P. Wilkes, T. B. Waltzek, D. L. Miller, and M. J. Gray. 2019. A highly invasive chimeric ranavirus can decimate tadpole populations rapidly through multiple transmission pathways. Ecological Modelling 410:108777.

Podgwaite, J. D., R. C. Reardon, G. S. Walton, L. Venables, and D. M. Kolodny-Hirsch. 1992. Effects of aerially applied Gypchek on gypsy moth (Lepidoptera: Lymantriidae) populations in Maryland woodlots. Journal of Economic Entomology 85:1136–1139.

Poulin, R. 2020. Meta-analysis of seasonal dynamics of parasite infections in aquatic ecosystems. International Journal for Parasitology 50:501–510.

Quinn, J. F., and A. E. Dunham. 1983. On hypothesis testing in ecology and evolution. American Naturalist 122:602–617.

Rasband, S. N. 2015. Chaotic dynamics of nonlinear systems. Courier Dover Publications, Mineola, NY.

Reilly, J. R., and B. D. Elderd. 2014. Effects of biological control on long-term population dynamics: identifying unexpected outcomes. Journal of Applied Ecology 51:90–101.

Reznick, D. N., J. Losos, and J. Travis. 2019. From low to high gear: there has been a paradigm shift in our understanding of evolution. Ecology Letters 22:233–244.

Roland, J., and P. D. Taylor. 1997. Insect parasitoid species respond to forest structure at different spatial scales. Nature 386:710–713.

Searle, C. L., M. H. Cortez, K. K. Hunsberger, D. C. Grippi, I. A. Oleksy, C. L. Shaw, S. B. de la Serna, C. L. Lash, K. L. Dhir, and M. A. Duffy. 2016. Population density, not host competence, drives patterns of disease in an invaded community. American Naturalist 188:554–566.

Skaller, P. M. 1985. Patterns in the distribution of gypsy moth (*Lymantria dispar*) (Lepidoptera: Lymantriidae) egg masses over an 11-year population cycle. Environmental Entomology 14:106–117.

Tobin, P. C., B. B. Bai, D. A. Eggen, and D. S. Leonard. 2012. The ecology, geopolitics, and economics of managing *Lymantria dispar* in the United States. International Journal of Pest Management 58:195–210.

Toju, H. 2011. Weevils and camellias in a Darwin's race: model system for the study of eco-evolutionary interactions between species. Ecological Research 26:239–251.

Turchin, P. 1990. Rarity of density dependence or population regulation with lags? Nature 344:660–663.

———. 2003. Complex population dynamics: a theoretical/empirical synthesis. Vol. 35. Princeton University Press, Princeton, NJ.

Varley, G. C., G. R. Gradwell, and M. P. Hassell. 1973. Insect population ecology: an analytical approach. Blackwell Scientific Publications, Oxford.

Wearing, H. J., P. Rohani, and M. J. Keeling. 2005. Appropriate models for the management of infectious diseases. PLoS Medicine 2:e174.

Webb, R., G. White, J. Podgwaite, V. D'Amico, J. Slavicek, J. Swearingen, B. Onken, and K. Thorpe. 2005. Comparison of aerially-applied Gypchek strains against gypsy moth (Lepidoptera: Lymantriidae) in the presence of an *Entomophaga maimaiga* epizootic. Journal of Entomological Science 40:446–460.

Williams, D. W., R. W. Fuester, W. W. Metterhouse, R. J. Balaam, R. H. Bullock, and R. J. Chianesei. 1991. Oak defoliation and population density relationships for the gypsy moth (Lepidoptera: Lymantriidae). Journal of Economic Entomology 84:1508–1514.

Williams, D. W., and A. M. Liebhold. 1995. Influence of weather on the synchrony of gypsy moth (Lepidoptera: Lymantriidae) outbreaks in New England. Environmental Entomology 24:987–995.

Woods, S. A., and J. S. Elkinton. 1987. Bimodal patterns of mortality from nuclear polyhedrosis-virus in gypsy-moth (*Lymantria-dispar*) populations. Journal of Invertebrate Pathology 50:151–157.

Woods, S. A., J. S. Elkinton, K. D. Murray, A. M. Liebhold, J. R. Gould, and J. D. Podgwaite. 1991. Transmission dynamics of a nuclear polyhedrosis virus and predicting mortality in gypsy moth (Lepidoptera:Lymantriidae) populations. Journal of Economic Entomology 84:423–430.

Yoshida, T., L. E. Jones, S. P. Ellner, G. F. Fussmann, and N. G. Hairston. 2003. Rapid evolution drives ecological dynamics in a predator-prey system. Nature 424:303–306.

Associate Editor: Nicole Mideo
Editor: Daniel I. Bolnick

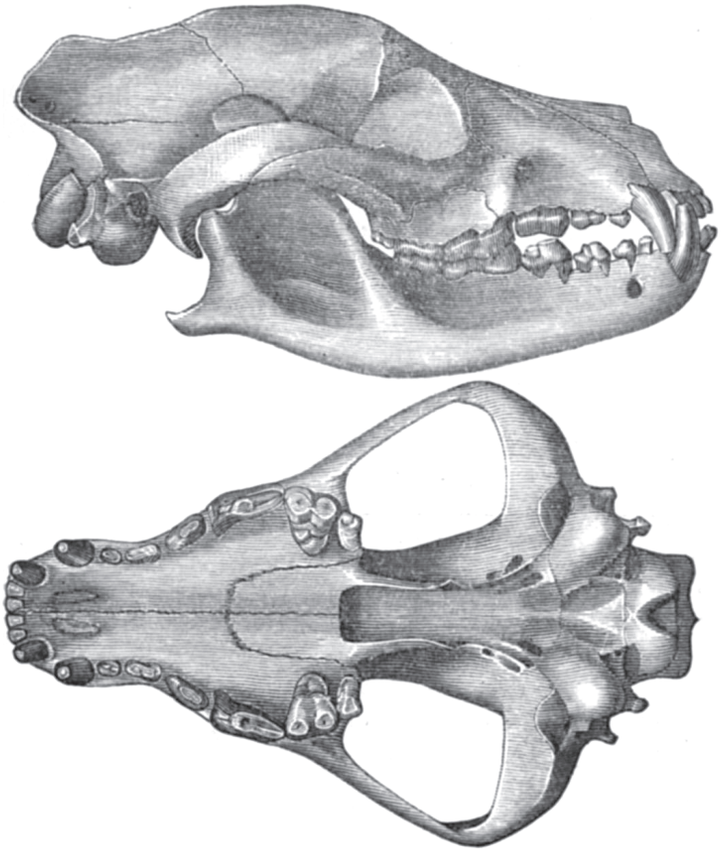

"Dr. Leidy described an *Ælurodon ferox*, whose affinities he did not determine, but which he thought to combine characters of dogs and cats. I have proven by material in my possession, that the *Ælurodon ferox* and the *Canis sævus* Leidy, are the same species. The genus Ælurodon must be referred to the Canidæ, and distinguished from Canis proper." From "On the Extinct Dogs of North America" by E. D. Cope (*The American Naturalist*, 1883, 17:235–249).